Thin Solid Films 520 (2012) 2211–2219

Contents lists available at SciVerse ScienceDirect

Thin Solid Films

journal homepage: www.elsevier.com/locate/tsf

Thin film formation at the air–water interface and on solid substrates of soluble axial substituted *cis*-bis-decanoate tin phthalocyanine

José Campos-Terán [a,*], Cristina Garza [b], Hiram I. Beltrán [c], Rolando Castillo [b]

[a] Departamento de Procesos y Tecnología, DCNI, Universidad Autónoma Metropolitana-Cuajimalpa, Artificios 40-sexto piso, Col. Hidalgo, D. F., 001120, Mexico
[b] Instituto de Física, Universidad Nacional Autónoma de México, P. O. Box 20-364, D. F., 01000, Mexico
[c] Departamento de Ciencias Naturales, DCNI, Universidad Autónoma Metropolitana-Cuajimalpa, Artificios 40-sexto piso, Col. Hidalgo, D. F., 001120, Mexico

ARTICLE INFO

Article history:
Received 1 March 2011
Received in revised form 10 October 2011
Accepted 27 October 2011
Available online 3 November 2011

Keywords:
Tin phthalocyanine
Thin films
Langmuir–Blodgett
Supramolecular assemblies
Atomic force microscopy
Brewster Angle Microscopy

ABSTRACT

Herein we study thin films of a recent kind of soluble axial substituted *cis*-bis-decanoate-tin^{IV} phthalocyanine (PcSn10) at the air/water interface, which were compressed isothermally and observed with Brewster Angle Microscopy. The air/water interfacial behavior of the films suggests that there are strong interactions among the PcSn10 molecules, which produces multilayers and 3D self-assemblies that prevent the formation of a Langmuir monolayer. Langmuir–Blodgett deposits of these films on both mica (negatively charged) and mild steel (positively charged) surfaces were developed. Information about the morphology of the film was obtained by using atomic force microscopy. We found structural differences in the PcSn10 thin films deposited on both substrates, suggesting that a combination of π–π, σ–π and Van der Waals interactions are the leading factors for the deposition, and consequently, for the control of supramolecular order. Our findings provide insights in the design of phthalocyanine molecules for the development of highly ordered and reproducible thin films.

1. Introduction

Phthalocyanines (Pc) are well known macrocyclic compounds which form ordered structures on different crystalline substrates [1,2]. These molecules are ideal for studies in fundamental and applied science [3], because their electronic and structural properties can be tuned by selective addition of a metal atom to the central cavity, or by modifying their macrocyclic Pc^{2-} molecular structure. Phthalocyanines (Pc) and their metallic derivatives (MPc; see Fig. 1) have been studied for their potential use as gas and liquid sensors [4–6], to improve storage devices such as DVDs and CDs [7,8], for solar cells [9,10], for liquid crystal displays [11,12], and as photosensitizers in photodynamic therapy for the treatment of varying diseases [13–17], among other applications [18]. Many of the mentioned applications rely on the production of Pc and MPc thin films, and on their supramolecular assemblies on surfaces. As a consequence, there is an actual interest in the deposition of these compounds on different substrates and the characterization of these deposits. In this sense, current research is focused on design of suitable compounds that enables the production of highly ordered and reproducible films.

Several techniques have been used to prepare thin films, such as vacuum deposition, which is one of the most common methods used to prepare inorganic thin films of an almost perfect structure [19–21]. On the other hand, wet-process techniques such as spin-coating [22] and layer by layer deposition [23,24] have attracted much attention because they are suitable for producing well ordered films with a low cost at ambient temperature and pressure. Another alternative method is Langmuir–Blodgett (LB) deposition [25–27], capable of producing highly ordered films of monomolecular thickness with dense packed structure. Since the pioneering works of Roberts et al. [28,29] as well as Snow [30] and Barger [31], over the past 25 years, a number of reports [32–41] have appeared dealing with the fabrication, characterization, and application of LB films using soluble Pc. Different molecular designs have been used with quite varied results [41–43]. Substitution of the metal core in the Pc is a design variable, as well as modifications of Pc with different hydrophobic groups in the eight outer, eight inner, or the whole sixteen positions at the isoindolinic moieties. In general, the LB films obtained by using these kinds of substitutions form arrangements where molecules are stacked in columnar assemblies mainly set up by strong molecular π–π interactions and in a lesser extent due to T-shaped σ-π interactions [41–43].

Recently, in our group there were synthesized a series of tin phthalocyanines (SnPc), in which owing to the preference of a tin atom to set bidentate linear carboxylate (from C6 to C18) moieties in *cis* disposition, resulted in SnPc compounds with a electron rich Pc face free of organic substituents. Meanwhile on the opposite face, it is located the Pc^{2-} ligand with two carboxylate fragments, [44,45] where this occupied face is partially crowded with hydrocarbon tails (see Fig. 1). This approach enhanced the solubility of this substituted SnPc in organic solvents, allowing their further spectroscopic characterization through

* Corresponding author. Tel.: +52 5526363800; fax: +52 5526363845.
E-mail address: jcampos@correo.cua.uam.mx (J. Campos-Terán).

0040-6090/$ – see front matter © 2011 Elsevier B.V. All rights reserved.
doi:10.1016/j.tsf.2011.10.155

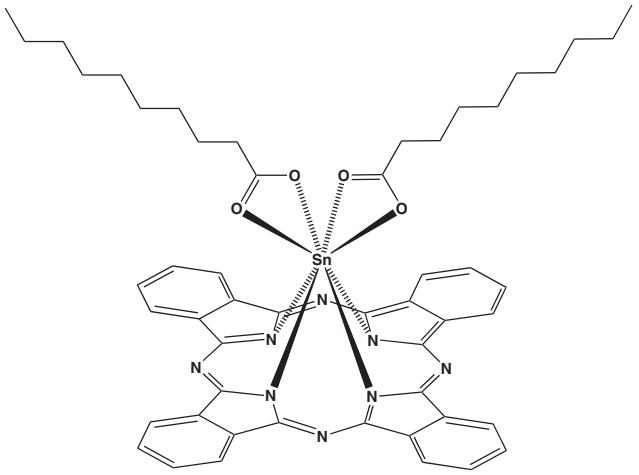

Fig. 1. Molecular structure of *cis*-bis decanoate tin phthalocyanine (PcSn10).

nuclear magnetic resonance (NMR), infrared (IR) and ultra violet-visible (UV–vis) spectroscopies, and X-ray diffraction analyses [44,45], which otherwise are unsuitable for most of the MPc. In particular, because of this enhanced solubility and their hypothesized capability to interact with a metallic surface through the naked electron rich Pc face, this dicarboxylate SnPc has been studied as a plausible corrosion inhibitor [44,45]. In this case, the hypothetical process of protection is that the metallic surface would be covered with the naked face of the Pc macrocycle besides receiving hydrophobic protection from the carboxylate tails. The results of corrosion inhibition activity have shown interesting tendencies [44,45]. However, there was not a clear picture of the surface absorption mechanism of these molecules on metallic substrates, *e.g. cis*-bis-decanoate-tin^{IV} phthalocyanine (PcSn10, see Fig. 1) has a concentration dependent corrosion inhibition behavior, stating that at 1000 ppm its efficiency is 58.8%, meanwhile at 500 ppm it augmented to 74.1%, which is counter sense to what is expected. For this reason, this specific compound has been chosen in this article as a subject of study for interfacial and surface studies.

In the present study, PcSn10 films at the air/water interface and the LB films transferred both on mica and mild steel are used to investigate how molecular structure correlates with the formation of thin films and with surface adsorption at negatively and positively charged substrates. At the air/water interface the films were compressed isothermally and observed with Brewster Angle Microscopy (BAM) [46,47], which allows monitoring the film formation, as well as, the compression process. This technique has been used to characterize monolayers of long chain carboxylic acids [48], porphyrins [49,50], phospholipids, mixtures among the latter two [51,52], and even protein monolayers [53,54]. In our case, it was not possible to obtain Langmuir monolayers from all the PcSn10/chloroform spreading solutions employed. However, reducing the solution concentration close to the monomolecular state, as was observed with UV–vis spectra, resulted in a film at the air/water interface with a homogeneous condensed phase. These PcSn10 films were transferred on mica and on mild steel surfaces by LB deposition, and subsequently, they were studied with atomic force microcopy (AFM). The present results indicated a difference in quality between the deposited films on both substrates, where it seems that mica negative electrostatic charge favors a better PcSn10 surface coverage.

2. Experimental work

2.1. Reagents

PcSn10 was synthesized through the microwave method reported by Beltran et al. [44,45] and characterized accordingly. Spectroscopic purity was determined using ^{1}H NMR, it was found to be *ca.* 99%. To increase this value, 0.5 g of PcSn10 was dissolved in 20 mL of high performance liquid chromatography (HPLC) chloroform. This solution was applied into a preparative alumina plate and eluted with HPLC chloroform. After Soxhlet extraction of the eluted fraction, evaporation under reduced pressure produced an increment in the purified compound as determined by thin layer chromatography using chloroform as eluent. The spreading solutions were made with chloroform (99% HPLC grade, Aldrich USA). The water subphase for the Langmuir films was ultrapure deionized water (Nanopure-UV, USA; 18.3 MΩ), which was filtered through a 0.22 μm membrane filter. UV–vis measurements of PcSn10 in chloroform solutions were carried out through scans from 190 to 1100 nm (bandwidth 0.5 nm) in absorbance mode using an Evolution 300 UV–vis spectrophotometer (Thermoscientific Inc, USA). Spectral process and analysis were recorded by using the vision Pro Thermo Electron UV–vis spectrometry software version 4.10.

2.2. Preparation of surfaces

The metal surfaces under investigation consisted of low carbon steel sheets of the type G10100 using the unified number system. The wt.% of impurities in Fe samples are: C = 0.08–0.13%, Si = 0.30–0.60%, Mn = 0.60–0.90%, P = 0.030% max., S = 0.035% max. Disk-shaped specimens of 11 mm diameter and 0.25 mm thickness were cut from an annealed steel sheet. Each sample was wet abraded with silicon carbide paper to 1200 grit finish, mechanically polished with alumina slurries (0.3 and 0.05 μm), and ultrasonically washed in deionized water; afterwards, samples were rinsed in acetone and ethanol, dried and kept in a desiccator before the experimental tests. Muscovite mica pieces of a size ~1 cm^2, for LB film deposition and AFM analysis, were freshly cleaved previous to the experiment. Before being used, both surfaces, mica and mild steel, were plasma cleaned by radio frequency-generated in air/H_2O plasma (~2 min at ~30 W, 13.33 Pa) in a Harrick Plasma Cleaner (PDC-23G, NY).

2.3. Films of PcSn10 at the air/water interface

Approximately 150–200 μL of a chloroform solution of PcSn10 (0.28 to 1.00 mg/mL) prepared the same day of the experiment was spread onto a water subphase (pH = 6.3) to form a film with an area per molecule ≥ 300 Å/molecule. After spreading the PcSn10 solution, a waiting time was needed until the pressure drop was negligible after solvent evaporation; typical waiting times were *ca.* 15 min. Compression isotherms of the PcSn10 films were done at a rate of 60 cm^2/min, on a computerized Nima LB trough (*TKB 2410A*, Nima Technology LTD, England) using a Wilhelmy plate to measure the lateral pressure, $\Pi = \gamma_o - \gamma$, i.e., the surface tension difference of the clean subphase, γ_o, and that of the PcSn10 covered subphase, γ. Temperature was kept constant at 21.0 ± 0.2 °C with the aid of a water circulator bath (Cole-Parmer *1268-24*, USA). All experiments were carried out in a dust-free environment. The film was observed with BAM during all the compression process.

2.4. LB films of PcSn10

The PcSn10 films were transferred from the air/water interface simultaneously to the mild steel disks and the mica surfaces, via the vertical dipping method at a low speed (~1.5 mm min^{-1}) by using the Nima LB trough mentioned above. The lateral pressure for transferring the monolayer was usually selected to be between 15 and 25 mN/m. AFM observations were performed just after preparation.

2.5. BAM

Air–water interface observations were performed in a BAM1 Plus (Nanofilm Technologie GmbH, Germany) with a spatial resolution *ca.* 4 μm. The BAM technique is based on the fact that the presence of a film at the air/water interface modifies the local parallel reflectivity of the interface, when illuminated with a parallel polarized He–Ne laser beam at the Brewster angle incidence (~53°). In this case, the microscope receives the reflected beam that is analyzed by a polarization analyzer. Afterwards, the signal is then received by a CCD video camera to develop an image of the film.

2.6. AFM observations

The PcSn10 LB films deposited on mica and on mild steel were analyzed with a JSTM-4210 JEOL (JEOL, Japan) scanning probe microscope with a 25×25 μm scanner. Samples under vacuum were observed operating in non-contact dynamic mode (intermittent contact) to obtain topographic and phase images. Non-contact silicon cantilevers (Mickomash, OR) with a typical force constant of 40 N/m were used. Calibration of the equipment was done by using calibrated gratings (Mickomash, OR) in vacuum and in ambient pressure, previous to each sample measurement. The images were analyzed by using the JEOL software.

3. Results and discussion

3.1. PcSn10 Langmuir films

Fig. 2 shows typical surface pressure vs. surface area (Π − A) isotherms at 21.0 ± 0.2 °C for PcSn10 films deposited on a water subphase, where different concentrations in the spreading solution were used. These isotherms are similar to those obtained with alkoxy copper phthalocyanine [55] and with amphiphilic octasubstituted phthalocyanines [56]. The measured isotherms of PcSn10 seem to have a similar form, but there are some clear differences. As we can see in Fig. 2, in each isotherm Π begins to increase at different area per molecule, A_o, to form something similar to a condensed phase as used in the language of Langmuir monolayers. This area density increases as the spreading solution concentration decreases, i.e., from A_o ~ 100 Å^2/molec for 1.00 mg/mL to A_o ~ 120 Å^2/molec for 0.28 mg/mL of PcSn10. These films become rigid in the range of ~60–80 Å^2/molec. Here, the compressibility of all films is approximately the same, with a typical compressibility ($\kappa = -1/A\ (\partial A/\partial \Pi)_T$) of ~2–5×10^{-2} m/mN. The limiting areas per molecule, A_{lim}, calculated by extrapolating the linear region of the isotherms to zero pressure, are around 70 Å^2/molec and 80 Å^2/molec for the developed films. The larger value is obtained for the less concentrated PcSn10 spreading solution.

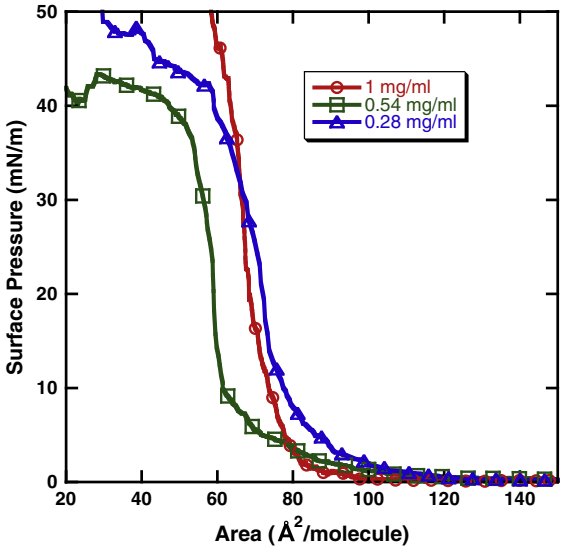

Fig. 2. Isotherms for PcSn10 films at the water/air interface, at 21.0 ± 0.2 °C, produced with three different spreading solution concentrations: (○) 1.00 mg/mL, (□) 0.54 mg/mL, (△) 0.28 mg/mL.

In general, the arrangements of the MPcs derivatives with organic substituents on the air/water interface must depend mainly on a balance between the combinations of Van der Waals, σ–π and π–π interactions among the MPc molecules, and the interactions of both, the surrounding ring planes as well as the organic substituents with the water surface. It has been found that when π–π interactions dominate, MPcs assemble into rod like columnar aggregates with the Pc planes edge-on over the air–water interface with a thickness corresponding to one Pc molecule [41–43]. On the contrary, if an MPc ring (with particular polar substituents) plane interaction with the water interface is stronger, then it will be placed with the aromatic rings laying flat upon the interface [42,43,56]. In addition, with some particular non polar substituents it has been found that the plane interaction with the water interface becomes weaker and the molecules could be slanted over it[41,43,55].

In our isotherms, A_{lim} values are smaller than the area occupied by the PcSn10 in the edge-on configuration, where the geometrical estimate would give molecular areas from A_{lim} ~ 112 to 250 Å^2/molec, depending on how the tails conformations are, namely, coiled, intercalated, or extended, respectively. On the other hand, a PcSn10 ring plane lying flat upon the air–water interface, would have a value near A_{lim} ~ 160 Å^2/molec, considering a rough geometrical estimate of the PcSn10 molecule. However, this will be a non-favorable conformation for PcSn10, since for this molecule there is another possible interaction to be considered among the molecules because of its reduced symmetry: the attractive tail–tail interaction (see Fig. 1). If this is the case, carboxylate tails would probably induce a more complicated conformation. Since our experimental A_{lim} are much lower than the geometrical edge-on or flat upon values, this suggests that the PcSn10 film is actually a multilayered structure. However, since it seems that A_{lim} increases when the PcSn10 spreading solution concentration decreases, apparently the out-of-interface molecular organization declines. Taking into account the above and since our experimental average A_{lim} is of 75 Å^2/molec a possible conformation will be to consider a bilayer structure where there is an inclined edge-on conformation maximizing the tail–tail interaction. Here, if we consider a 160 Å^2/molec as the area occupied by the PcSn10 ring plane, this will give us an angle of inclination of approximately 46.7° (see Fig. 3).

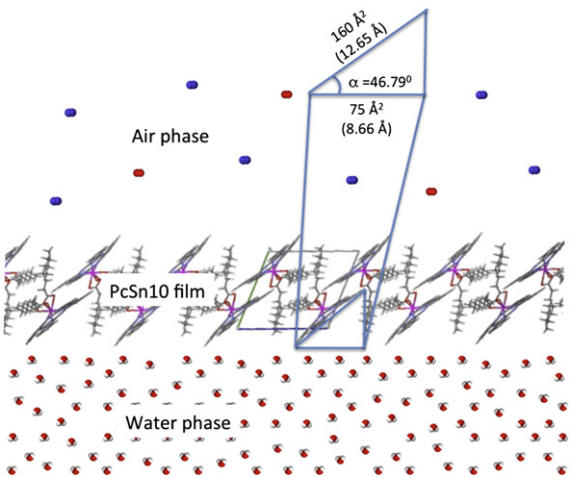

Fig. 3. A possible model for the structure of a PcSn10 thin film at the air/water interface, where only a bilayer is presented.

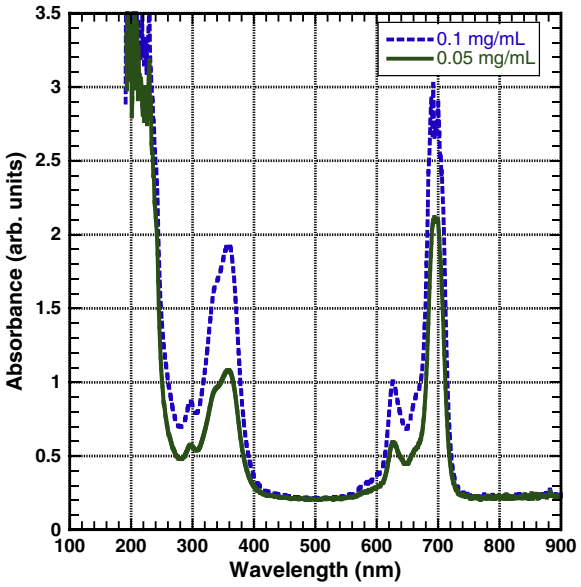

Fig. 4. UV–vis measurements at different PcSn10/chloroform solution concentrations.

To estimate how molecular interactions could affect the assembly of PcSn10 molecules in solution, we performed UV–vis measurements at 0.1 and 0.05 mg/mL PcSn10-chloroform solution concentrations. The comparison of UV–vis spectra at these different concentrations has been performed just in order to ascertain PcSn10 aggregation behavior. The locations and shape of the Q-band (at ~680 nm) can be used to estimate the aggregation behavior of MPc [57]. As we can observe in Fig. 4, both UV–vis spectra present absorption bands between 630 and 680 nm, which are similar to the ones found for ZnPc [40,43]. These bands become more defined in the absorption bandwidth and with less absorbance at the lower concentration (0.05 mg/mL). This indicates that at low concentrations, the assemblies have a small number of molecules, getting close to a single molecule state. Hence, at the air–water interface, it is worth noticing that we are not spreading single PcSn10 molecules but some type of aggregates.

BAM is a powerful technique that allows characterizing films formation at the air/water interface without perturbing it. Tilting order phases have been described with this technique [48]. BAM observations have been done for metalloporphyrins [50] and in very few cases for Pc compounds [58]. In Fig. 5, we observe BAM images of PcSn10 Langmuir films obtained after depositing PcSn10 using different spreading solution concentrations. The images present films at different area densities and at different lateral pressures. The effect of varying the spreading solution concentration on the films is clearly visible. Initially, we will describe the BAM images when the spreading solution is concentrated (1.00 mg/mL, Fig. 5a–c). In Fig. 5a, we observe a uniform film in dark gray and almost triangular shaped black domains that are thick micrometric crystals of PcSn10, which form and grow almost immediately after the PcSn10/chloroform solution is spread on the water surface ($\Pi \sim 0$ mN/m). Fluid motion around these objects confirms their solid character. In general, dark and bright regions in BAM images correspond to phase coexistence in the films. One of them usually is similar to a two dimensional monolayer gas phase (dark) and another to a monolayer condensed phase (bright). Consequently, crystals should be very bright when observed with BAM as it is usual in solids films at air/water interface. The large reflectivity is due to their high density and thickness.

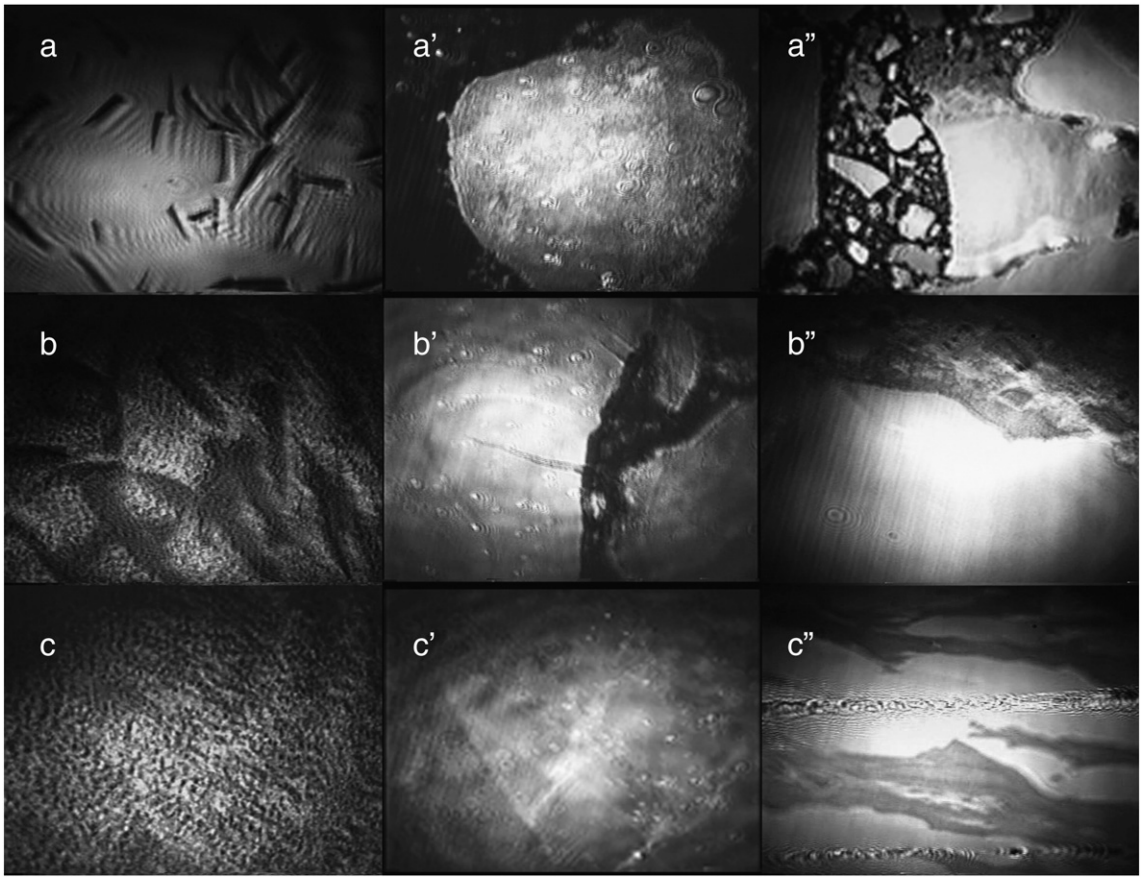

Fig. 5. BAM images for PcSn10 films at the water–air interface. In the columns, images where different spreading solution were used: a–c) 1 mg/mL. a′–c′) 0.54 mg/mL. a″–c″) 0.28 mg/mL. In the rows we present images of the film at different lateral pressures: a, a′, a″, b, and b′) At $\Pi \sim 0$ mN/m. b″) At $\Pi = 15$ mN/m. c) At $\Pi = 43$ mN/m. c′) At $\Pi = 32$ mN/m. c″) Collapse. The horizontal breadth corresponds to 850 μm.

Curiously, in our case crystals are particularly dark. The most adequate explanation for this irregular observation is related to the nature of the PcSn10 molecules that form the crystals, which clearly absorb light at *ca.* 600–700 nm (see Fig. 4) and hence absorb the light from the laser beam coming from the microscope (HeNe laser, λ ~ 632 nm) resulting in black defined structures; here, as crystals thicken the light absorption is larger, as observed from the spectra of Fig. 4. The formation of these crystals is not unexpected, because relatively big aggregates are already present in the chloroform spreading solution, as noticed in the UV–vis spectra of Fig. 4. Then, when the PcSn10 molecules are spread on the air/water interface, in principle they would avoid interacting with the water phase by forming big clusters that maximize their hydrophobic interactions and thus minimize the energy of the system. In fact as time elapses, and even without compressing the film, the texture of the film changes, and apparently subsequent PcSn10 layers cover the crystals (see Fig. 5b), which grow forming a film that seems to be corrugated. When the film is compressed, these changes are enhanced forming a film not really homogeneous, where different intensities are observed in the image indicating that a multilayer is formed (see Fig. 5c). By reducing the PcSn10 concentration in the spreading solution to 0.54 mg/mL, fewer aggregates are present and thinner films without micro-crystals are obtained as observed in Fig. 5a′. In addition, here there are regions that are very similar to a monolayer gas phase (black areas in Fig. 5a′–b′). Nevertheless, many Fraunhofer rings [59] along bright domains of something similar to a condensed phase reveal the presence of material outside the interface, i.e., the film is not a monolayer. On compression, the gas phase continuously decreases until a film covers all the field of view. However, there are clear indications of material expelled, since we still observe Fraunhofer rings and domains with large reflectivity, which are indications of a multilayer process in the film (see Fig. 5c′). The film with the best quality is the one produced from the 0.28 mg/mL solution that is shown in Fig. 5a″–c″. Here, we do not observe aggregates at this resolution, instead a homogeneous condensed phase is observed in

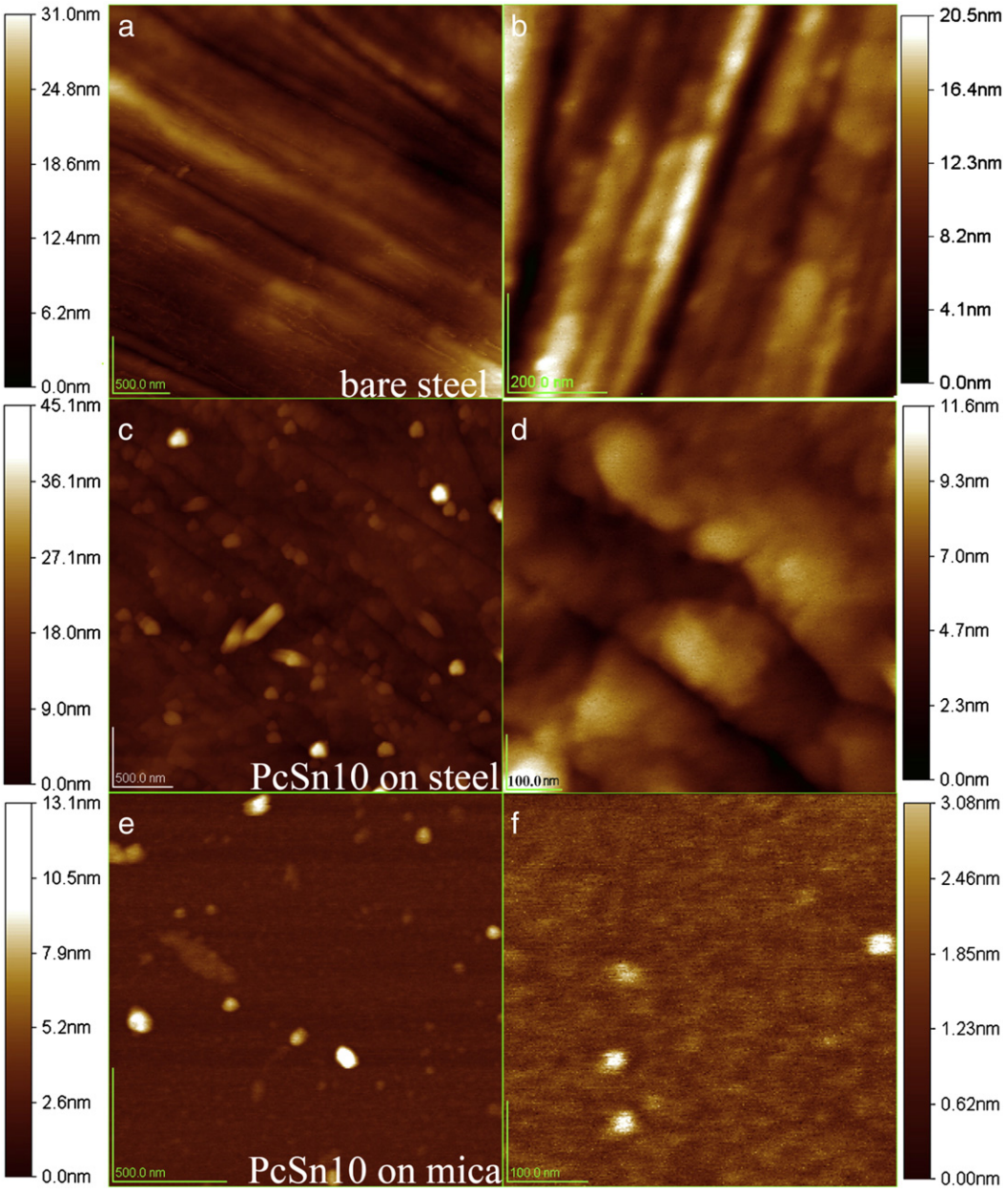

Fig. 6. AFM intermittent contact topographic images of: (a) bare mild steel, (c) PcSn10 LB films deposited on mild steel and(e) PcSn10 deposited on mica. b, d, and f) Measured amplifications of the films at the left column, respectively. Films were deposited at 22 mN/m from a 1 mg/mL solution.

coexistence with a film that is quite fluid and similar to a gas phase in monolayers. At 15 mN/m, the film is in the condensed phase region showing big homogeneous domains with the same brightness, which indicates that the film has approximately the same thickness (Fig. 5b″). When this film gets to the collapse, brighter and darker regions are present that indicates regions with different thickness, see Fig. 5c″. In general, all the LB deposits were made close to this surface pressure.

3.2. AFM observations of PcSn10 LB films

In Figs. 6, 7, and 8, we present AFM images of PcSn10 films LB transferred on mica and on mild steel where spreading solutions with different concentration were used to make the film at the air/water interface. Fig. 6a and b presents topographic images of bare mild steel revealing something like rough stripes that correspond to the groves in the metal due to the polishing process (roughness ~ 3 nm). In Fig. 6c we present contact mode topographic images of a PcSn10 film deposited on mild steel at Π ~ 22 mN/m from a film made with a 1.00 mg/mL spreading solution, and in Fig. 6d we present an amplification made on the same film presented in 6c. Fig. 6c and d shows the deposit of PcSn10 on mild steel following the roughness of the metal. However, the quality of the film is relatively poor due to the presence of large aggregates or small crystals of PcSn10. If the large aggregates are not taken into account, the roughness of both films is almost the same (~1.4 nm), which is lower than the roughness found in mild steel. In Fig. 6e and f, we present AFM images of a PcSn10 LB film deposited on mica, which was LB transferred simultaneously with the mild steel samples just described. For mica surfaces, we observe approximately the same features than in the metal deposit, except that they do not present the underlying roughness of the metal. Here, we observe a film with large aggregates over it that is similar to what we called the condensed phase in the film at the air/water interface. The roughness in this case, without considering the big aggregates, is quite low (~0.3 nm).

In Fig. 7a and b, we observe a PcSn10 film LB transferred on mild steel at a Π ~ 10 mN/m, from a film made with a 0.54 mg/mL spreading solution. In the inset of Fig. 7a, we present a 15 × 15 μm image, showing the transferred film covering the metal surface with aggregates along all the field of view. a and b of Fig. 7 are actual amplifications of the film observed in the inset of Fig. 7a. Here, we can observe that these aggregates form clusters along the surface. Why these aggregates are formed on mild steel is not clear yet. A possibility could be related to the formation of clusters in the film at the air/water interface. Once the film is deposited on the metal surface, the interaction between the members of the aggregates does not allow them to disassemble to form a uniform film over the metal surface. Therefore, the interaction among PcSn10 molecules apparently is larger than that between the PcSn10 molecule and mild steel. The roughness of the covering film in this case is ~26 nm, which is much larger than the roughness of the films presented in Fig. 6. In contrast, when the film was LB transferred onto mica (Fig. 7c), the transferred film seems to be more smooth and flat, although it presents small aggregates. In addition, it is not strange to find two kinds of regions with a height difference between them of ~0.45 nm (see Fig. 7d). These in-homogeneities probably correspond to regions with bad coverage in the original film at the air/water interface.

In Fig. 8a, we observe a PcSn10 film LB transferred on mild steel at Π ~ 15 mN/m, which was made with a 0.28 mg/mL spreading solution. In this case, the film seems to be homogeneous and apparently covers the metal surface up to ~100%, but without masking the grooved surface of mild steel. The film maintains almost the original roughness of the bare mild steel, which is 2.2 nm. The phase lag image of the film (Fig. 8b), reveals that it is formed by two kinds of domains probably structured differently. In Fig. 8c, we present two images of the PcSn10 film but now LB transferred onto mica (figure 2 × 2 μm and inset 2.6 × 2.6 μm). Here, we observe a flat film with irregular domains on it, which presents different sizes and almost the same height. The inset in Fig. 8c shows a different area of the covered

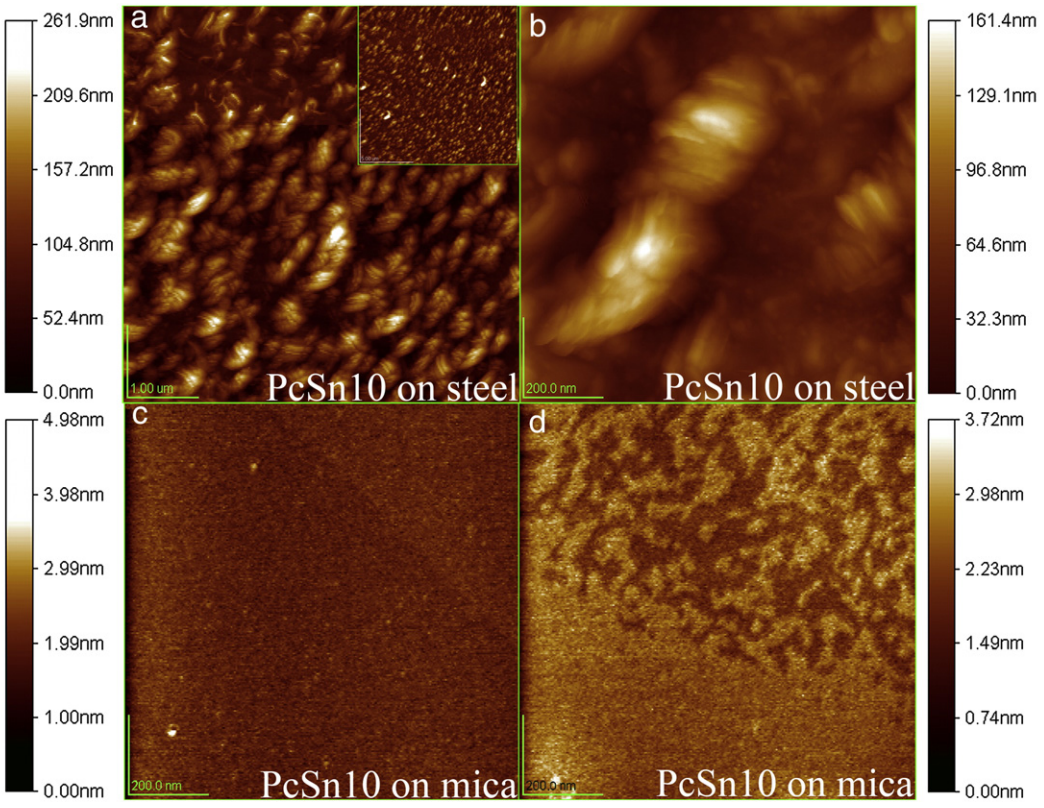

Fig. 7. AFM intermittent contact topographic images of PcSn10 LB films deposited on mild steel or mica at 10 mN/m from a 0.54 mg/mL solution.

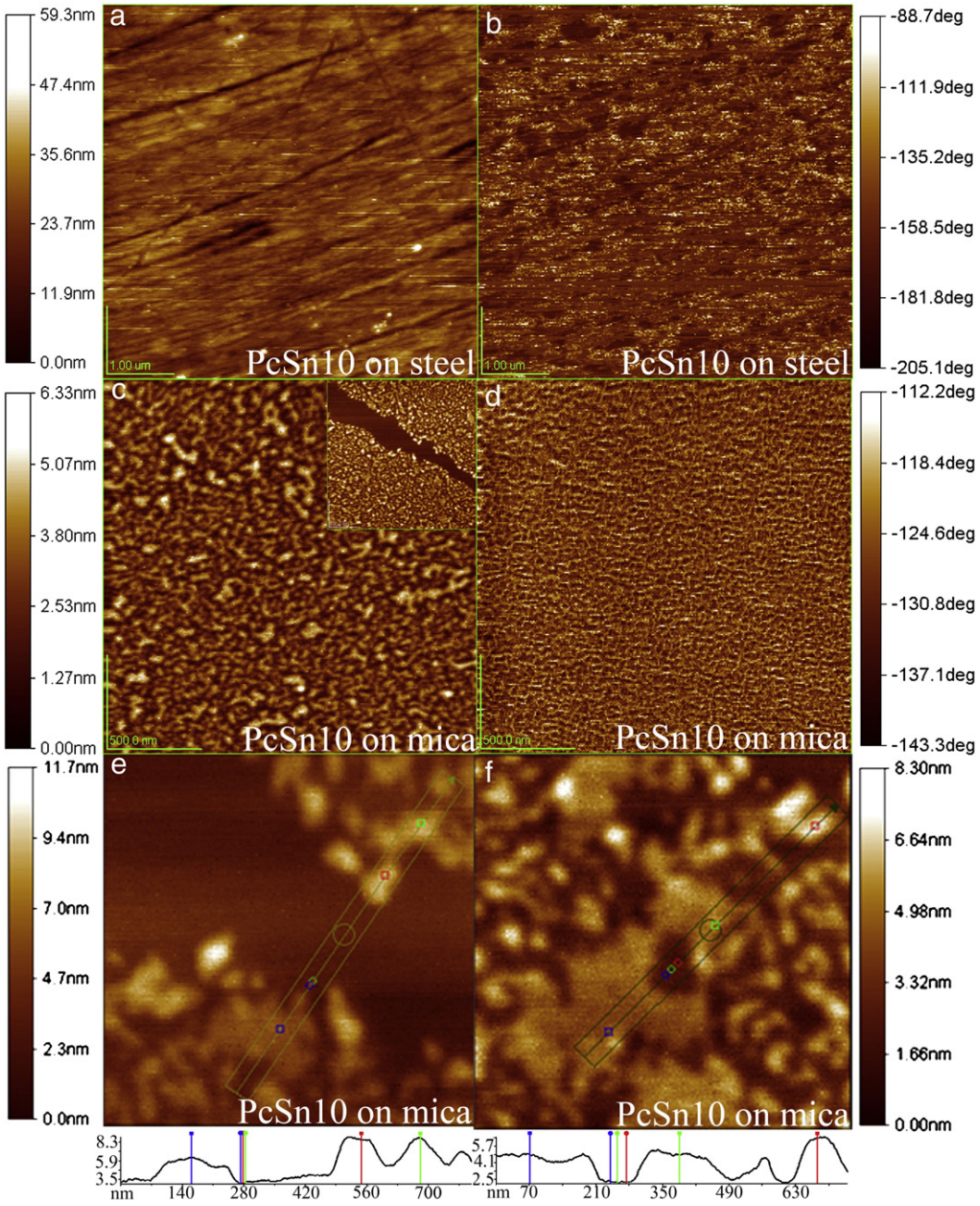

Fig. 8. AFM intermittent contact topographic and phase images of PcSn10 LB films deposited on mild steel (a, b) and mica (c, d) at 15 mN/m from a 0.28 mg/mL solution. Image from another location (inset) and typical line height data is presented for the film deposited on mica. e and f) Amplifications of Fig. 8c, and averaged topographic profiles at specific points on the wide line indicated in the figures.

mica surface, where we found a homogenous large dark area coexisting with the film with irregular domains. Fig. 8d presents a phase lag image of the film depicted in Fig. 8c, where we observe an irregular network arrangement with an intricate texture, revealing that the domains determined by the topographic images have a different structure. Apparently, in this case the films at mica and mild steel surfaces behave in the same way, but the roughness in the mild steel do not allow to appreciate if they have the same structural quality. e and f in Fig. 8 present averaged topographic profiles using a wide line, over perpendicular sections at specific locations of Fig. 8c. Fig. 8e presents an image corresponding to the gap observed in the inset of Fig. 8c, and the height profile along this gap. Clearly, we observe that the dark areas in the images are not bare mica, because they appear slightly covered as revealed by the slope in the profile, and apparently, all the irregular bright domains are above that level. On the average the height difference between these two levels is ~5 nm. This is a clear indication that these irregular domains are made of multilayers. In Fig. 8f, we present another image of a region in Fig. 8c with many domains and a height profile. As in Fig. 8e, there are bright domains that are taller than the dark domains. The dark domains approximately have the same level of coverage along the entire image and seem to correspond to what we called as the gas phase in the film generated at the air/water interface. In the same way, the tall domains seem to correspond to what we called the condensed phase, which actually are 3D multilayers. In this image, the difference between both levels (dark and bright domains) is ~3.1 nm.

The results obtained through the analysis of the compression isotherms, BAM and AFM images give some insight of the PcSn10 interfacial adsorption process. Initially, although the air/water interface could have played an important role in the displacement of

the PcSn10 bulk cluster size assembly equilibrium, this was not clearly observed. In addition, the different films produced showed different PcSn10 cluster sizes that must probably corresponded to the original ones that were present in the different spreading solutions used. Hence, it seems that up to this point the PcSn10 molecules maximize their π–π, σ–π and Van der Waals interactions and thus minimize the energy of the system by keeping their actual cluster formation avoiding their interaction with the water phase (see Fig. 3). These interactions seem to be present even when these films were transfer onto solid substrates (see for example Figs. 6c, 7a and 8a). However, we do observe a difference in quality between the films on mica and on mild steel surfaces where it seems that mica favors a better surface coverage by the film. This behavior could be related to the different electrostatic charge nature of the surfaces. In one case, there is a repulsive electrostatic interaction due to the dipole and quadrupolar character of the PcSn10 molecules and the high negative charge density on mica (0.3 C/m^2 or one charge per 0.5 nm^2) [60,61]. In the second case, there is an attractive interaction between the PcSn10 molecules and the positive charge of the mild steel surface [62]. The interaction in the former case apparently is larger than in the latter. Even that it sounds contradictory that PcSn10-mica repulsive interaction favors a better surface coverage by the film, what is most probably happening is that in order to avoid electronic repulsion the aromatic rings on the PcSn10 molecules are a little bit displaced with respect to the surface negative charges, and hence they form a stable layer of aromatic rings in close contact with the mica surface. An analog example of this situation is present in graphite layers [63,64] and in the stabilization of graphene composites [65,66].

4. Conclusions

The interfacial behavior of PcSn10 thin films on the air/water interface, mica (negatively charged) and mild steel (positively charged) surfaces suggests that although PcSn10 molecules were axially functionalized to reduce the strong π–π interactions present in non-substituted Pc, they still produce multilayers and 3D self-assemblies preventing the formation of monomolecular films. In addition, although the air/water interface could have played an important role in the displacement of the PcSn10 bulk cluster size assembly equilibrium, this was not clearly observed. On the other hand, structural differences in the PcSn10 thin films deposited on mica and on mild steel, suggests that combinations of electrostatic (with the surface) and Van der Waals, σ–π and π–π interactions (among the PcSn10 molecules) are the leading factors for the deposition, and consequently, for the control of supramolecular order. From the application point of view, an important surface coverage is accomplished during LB deposition using a low PcSn10 spreading solution concentration, indicating that is possible to have a PcSn10 thin film that can interact with different surfaces. Taking into account our results, PcSn10 molecule is a good starting point in the molecular design of axially substituted phthalocyanines for the development of highly ordered and reproducible thin films.

Acknowledgments

The financial support from TWAS (06-299 RG/PHYS/LA), UAM (Acuerdo 11/2007), SEP-CONACYT (81081) and DGAPA-UNAM (104911) are gratefully acknowledged. We thank Maribel Hernández for her help with UV–vis measurements and Salvador Ramos for his technical assistance with BAM.

References

[1] X.H. Qiu, C. Wang, Q.D. Zeng, B. Xu, S.X. Yin, H.N. Wang, S.D. Xu, C.L. Bai, J. Am. Chem. Soc. 122 (2000) 5550.
[2] T.G. Gopakumar, M. Lackinger, M. Hackert, F. Muller, M. Hietschold, J. Phys. Chem. B 108 (2004) 7839.
[3] H. Engelkamp, S. Middelbeek, R.J.M. Nolte, Science 284 (1999) 785.
[4] M. Masui, M. Sasahara, T. Wada, M. Takeuchi, Appl. Surf. Sci. 92 (1996) 643.
[5] J.C. Hsieh, C.J. Liu, Y.H. Ju, Thin Solid Films 322 (1998) 98.
[6] N. Kilinc, D. Atilla, S. Ozturk, A.G. Gurek, Z.Z. Ozturk, V. Ahsen, Thin Solid Films 517 (2009) 6206.
[7] R. Ao, L. Kummerl, D. Haarer, Adv. Mater. 7 (1995) 495.
[8] D.H. Gu, Q.Y. Chen, J.P. Shu, X.D. Tang, F.X. Gan, S.Y. Shen, K. Liu, H.J. Xu, Thin Solid Films 257 (1995) 88.
[9] S. Siebentritt, S. Gunster, D. Meissner, Synth. Met. 41 (1991) 1173.
[10] D. Wohrle, D. Meissner, Adv. Mater. 3 (1991) 129.
[11] M.M. Ayhan, M. Durmus, A.G. Gurek, J. Porphyrins Phthalocyanines 13 (2009) 722.
[12] H. Mukai, K. Hatsusaka, K. Ohta, J. Porphyrins Phthalocyanines 13 (2009) 927.
[13] S.A. Priola, A. Raines, W.S. Caughey, Science 287 (2000) 1503.
[14] M.E. Rodriguez, P. Zhang, K. Azizuddin, G.B. Delos Santos, S.M. Chiu, L.Y. Xue, J.C. Berlin, X.Z. Peng, H.Q. Wu, M. Lam, A.L. Nieminen, M.E. Kenney, N.L. Oleinick, Photochem. Photobiol. 85 (2009) 1189.
[15] G.R. Lamberto, A. Binolfi, M.L. Orcellet, C.W. Bertoncini, M. Zweckstetter, C. Griesinger, C.O. Fernandez, PNAS 106 (2009) 21057.
[16] P.A. Barbugli, M.P. Siqueira-Moura, E.M. Espreafico, A.C. Tedesco, J. Nanosci. Nanotechnol. 10 (2010) 569.
[17] K. Ishii, M. Shiine, Y. Shimizu, S.-i. Hoshino, H. Abe, K. Sogawa, N. Kobayashi, J. Phys. Chem. B 112 (2008) 3138.
[18] C.C. Leznoff, A.B.P. Lever (Eds.), Phthalocyanines: Properties and Applications, VCH, New York, 1989.
[19] M. Lackinger, M. Hietschold, Surf. Sci. 520 (2002) L619.
[20] S. Kment, P. Kluson, M. Drobek, R. Kuzel, I. Gregora, M. Kohout, Z. Hubicka, Thin Solid Films 517 (2009) 5274.
[21] M. Krzywiecki, L. Ottaviano, L. Grzadziel, P. Parisse, S. Santucci, J. Szuber, Thin Solid Films 517 (2009) 1630.
[22] T. Komino, M. Matsuda, H. Tajima, Thin Solid Films 518 (2009) 688.
[23] C. Woojung, M. Naito, R. Fujii, M. Morisue, M. Fujiki, Thin Solid Films 518 (2009) 625.
[24] H. Benten, N. Kudo, H. Ohkita, S. Ito, Thin Solid Films 517 (2009) 2016.
[25] G. Roberts, Langmuir–Blodgett Films, Plenum Press, New York, 1990.
[26] A. Ulman, An Introduction to Ultrathin Organic Films: From Langmuir–Blodgett to Self-Assembly, Academic Press, San Diego, 1991.
[27] A. Ulman, Chem. Rev. 96 (1996) 1533.
[28] S. Baker, M.C. Petty, G.G. Roberts, M.V. Twigg, Thin Solid Films 99 (1983) 53.
[29] G.G. Roberts, M.C. Petty, S. Baker, M.T. Fowler, N.J. Thomas, Thin Solid Films 132 (1985) 113.
[30] A.W. Snow, N.L. Jarvis, J. Am. Chem. Soc. 106 (1984) 4706.
[31] W.R. Barger, A.W. Snow, H. Wohltjen, N.L. Jarvis, Thin Solid Films 133 (1985) 197.
[32] M.J. Cook, J. Mater. Chem. 6 (1996) 677.
[33] D.J. Revell, I. Chambrier, M.J. Cook, D.A. Russell, J. Mater. Chem. 10 (2000) 31.
[34] M.J. Cook, I. Chambrier, G.F. White, E. Fourie, J.C. Swarts, Dalton Trans. (2009) 1136.
[35] N. Kobayashi, H. Lam, W.A. Nevin, P. Janda, C.C. Leznoff, T. Koyama, A. Monden, H. Shirai, J. Am. Chem. Soc. 116 (1994) 879.
[36] M. Kimura, H. Ueki, K. Ohta, K. Hanabusa, H. Shirai, N. Kobayashi, Langmuir 18 (2002) 7683.
[37] P.E. Smolenyak, E.J. Osburn, S.Y. Chen, L.K. Chau, D.F. Obrien, N.R. Armstrong, Langmuir 13 (1997) 6568.
[38] C.L. Donley, W. Xia, B.A. Minch, R.A.P. Zangmeister, A.S. Drager, K. Nebesny, D.F. O'Brien, N.R. Armstrong, Langmuir 19 (2003) 6512.
[39] N. Kumaran, C.L. Donley, S.B. Mendes, N.R. Armstrong, J. Phys. Chem. C 112 (2008) 4971.
[40] L. Gaffo, V. Zucolotto, M.R. Cordeiro, W.C. Moreira, O.N. Oliveira, F. Cerdeira, M. Brasil, Thin Solid Films 515 (2007) 7307.
[41] P. Smolenyak, R. Peterson, K. Nebesny, M. Torker, D.F. O'Brien, N.R. Armstrong, J. Am. Chem. Soc. 121 (1999) 8628.
[42] M.J. Cook, Pure Appl. Chem. 71 (1999) 2145.
[43] M. Kimura, H. Ueki, K. Ohta, H. Shirai, N. Kobayashi, Langmuir 22 (2006) 5051.
[44] H.I. Beltran, R. Esquivel, A. Sosa-Sanchez, J.L. Sosa-Sanchez, H. Hopfl, V. Barba, N. Farfan, M.G. Garcia, O. Olivares-Xometl, L.S. Zamudio-Rivera, Inorg. Chem. 43 (2004) 3555.
[45] H.I. Beltran, R. Esquivel, M. Lozada-Cassou, M.A. Dominguez-Aguilar, A. Sosa-Sanchez, J.L. Sosa-Sanchez, H. Hopfl, V. Barba, R. Luna-Garcia, N. Farfan, L.S. Zamudio-Rivera, Chem. Eur. J. 11 (2005) 2705.
[46] S. Henon, J. Meunier, Rev. Sci. Instrum. 62 (1991) 936.
[47] D. Hoenig, D. Moebius, J. Phys. Chem. 95 (1991) 4590.
[48] S. Ramos, R. Castillo, J. Chem. Phys. 110 (1999) 7021.
[49] J.M. Pedrosa, C.M. Dooling, T.H. Richardson, R.K. Hyde, C.A. Hunter, M.T. Martin, L. Camacho, Langmuir 18 (2002) 7594.
[50] K. Noworyta, R. Marczak, R. Tylenda, J.W. Sobczak, R. Chitta, W. Kutner, F. D'Souza, Langmuir 23 (2007) 2555.
[51] I. Prieto, M.T.M. Romero, L. Camacho, D. Mobius, Langmuir 14 (1998) 4175.
[52] M. Perez-Morales, J.M. Pedrosa, M.T. Martin-Romero, D. Mobius, L. Camacho, J. Phys. Chem. B 108 (2004) 4457.
[53] J. Xicohtencatl-Cortes, J. Mas-Oliva, R. Castillo, J. Phys. Chem. B 108 (2004) 7307.
[54] V.M. Bolanos-Garcia, J. Mas-Oliva, S. Ramos, R. Castillo, J. Phys. Chem. B 103 (1999) 6236.
[55] T. Oshiro, A. Backstrom, A.M. Cumberlidge, K.W. Hipps, U. Mazur, S.P. Pevovar, D.F. Bahr, J. Smieja, J. Mater. Res. 19 (2004) 1461.

[56] M.J. Cook, J. McMurdo, D.A. Miles, R.H. Poynter, J.M. Simmons, S.D. Haslam, R.M. Richardson, K. Welford, J. Mater. Chem. 4 (1994) 1205.
[57] M.J. Stilman, T. Nyokong, in: C.C. Leznoff, A.B.P. Lever (Eds.), Phthalocyanines: Properties and Applications, vol. 1, VCH, New York, 1989, p. 133.
[58] F. Peñacorada, J. Souto, S. Katholy, J.A. de Saja, J. Reiche, Mater. Sci. Eng., C 5 (1998) 293.
[59] J. Galvan-Miyoshi, R. Castillo, J. Phys. Condens. Matter 14 (2002) 4767.
[60] J.N. Israelachvili, Intermolecular and Surface Forces, Academic Press, San Diego, CA, 1991.
[61] G.L. Gaines, J. Phys. Chem. 61 (1957) 1408.
[62] S. Ramachandran, V. Jovancicevic, Corrosion 55 (1999) 259.
[63] Y. Gogotsi, J.A. Libera, N. Kalashnikov, M. Yoshimura, Science 290 (2000) 317.
[64] G. Zhang, X. Jiang, E. Wang, Science 300 (2003) 472.
[65] A.J. Patil, J.L. Vickery, T.B. Scott, S. Mann, Adv. Mater. 21 (2009) 3159.
[66] Q. Su, S. Pang, V. Alijani, C. Li, X. Feng, K. Müllen, Adv. Mater. 21 (2009) 3191.